

**Please cite the Published Version**

Barr, ID, Ely, JC, Spagnolo, M, Clark, CD, Evans, IS, Pellicer, XM, Pellitero, R and Rea, BR (2017) Climate patterns during former periods of mountain glaciation in Britain and Ireland: Inferences from the cirque record. *Palaeogeography, Palaeoclimatology, Palaeoecology*, 485. pp. 466-475. ISSN 0031-0182

**DOI:** <https://doi.org/10.1016/j.palaeo.2017.07.001>

**Publisher:** Elsevier

**Version:** Accepted Version

**Downloaded from:** <https://e-space.mmu.ac.uk/619012/>

**Usage rights:**  [Creative Commons: Attribution-Noncommercial-No Derivative Works 4.0](https://creativecommons.org/licenses/by-nc-nd/4.0/)

**Additional Information:** This is an Author Accepted Manuscript of a paper accepted for publication in *Palaeogeography, Palaeoclimatology, Palaeoecology*, published by and copyright Elsevier.

**Enquiries:**

If you have questions about this document, contact [openresearch@mmu.ac.uk](mailto:openresearch@mmu.ac.uk). Please include the URL of the record in e-space. If you believe that your, or a third party's rights have been compromised through this document please see our Take Down policy (available from <https://www.mmu.ac.uk/library/using-the-library/policies-and-guidelines>)

1 **Climate patterns during former periods of mountain glaciation in Britain and Ireland:**  
2 **inferences from the cirque record**

3

4 Iestyn D Barr<sup>a\*</sup>, Jeremy C. Ely<sup>b</sup>, Matteo Spagnolo<sup>c,d</sup>, Chris D Clark<sup>b</sup>, Ian S Evans<sup>e</sup>, Xavier M Pellicer<sup>f</sup>,  
5 Ramón Pellitero<sup>c</sup>, Brice R Rea<sup>c</sup>

6

7 <sup>a</sup>School of Natural and Built Environment, Queen's University Belfast, Belfast, BT7 1NN, UK

8 <sup>b</sup>Department of Geography, The University of Sheffield, Sheffield, S10 2TN, UK

9 <sup>c</sup>School of Geosciences, University of Aberdeen, Aberdeen, AB24 3UF, UK

10 <sup>d</sup>Department of Earth and Planetary Science, University of California at Berkeley, Berkeley, CA 94709,

11 USA

12 <sup>e</sup>Department of Geography, University of Durham, Durham, UK, DH1 3LE, UK

13 <sup>f</sup>Geological Survey Ireland, Beggars Bush, Haddington Road, Dublin, Ireland

14

15 \*Corresponding author. Tel: 44(0)28 9097 5146; Email: i.barr@qub.ac.uk

16

17 **Abstract**

18 We map glacial cirques, and analyse spatial variability in their altitude and aspect to derive a  
19 long-term, time-integrated, perspective on climate patterns during former periods of mountain  
20 glaciation (likely spanning multiple Quaternary glaciations) in Britain and Ireland. The data reveal that,  
21 although air temperatures were important, exposure to moisture-bearing air masses was the key factor  
22 in regulating sites of former mountain glacier formation, and indicate that during such periods, moisture  
23 supply was largely controlled by North Atlantic westerlies, with notable inland precipitation gradients  
24 (precipitation decreasing inland), similar to present day. In places, trends in cirque altitude may also  
25 reflect regional differences in the extent of cirque deepening, controlled by the dimensions and  
26 dynamics of the glaciers that came to occupy them. Specifically, comparatively deep cirques in coastal  
27 locations may reflect the former presence of dynamic (fed by moisture from the North Atlantic), but  
28 comparatively small, glaciers (largely confined to their cirques). By contrast, decreasing cirque depth

29 further inland, may reflect the former presence of larger and/or less dynamic ice masses, occupying  
30 comparatively continental climatic conditions.

31

## 32 **Keywords**

33 Quaternary; glaciation; NE Atlantic; precipitation; glacial cirque

34

## 35 **1. Introduction**

36 The synoptic climate of Britain and Ireland (Fig. 1) is dominated by the interaction of polar and  
37 tropical air masses, and the mid-latitude westerlies that form at their boundary (Hurrell and Deser,  
38 2010). The key variable in determining the region's climate is therefore the position, stability and  
39 strength of this boundary, marked by the polar front jet stream (PFJS: a high-altitude band of strongest  
40 air-flow within the zone of mid latitude westerlies). At present, the average track of the PFJS is to the  
41 north of Scotland, meaning that Britain and Ireland lie in the direct path of mid-latitude moisture-  
42 bearing westerlies. This results in strong W–E precipitation gradients, which, in Britain, are subject to  
43 notable orographic enhancement, since much of the high ground is towards the North and West (Mayers  
44 and Wheeler, 2013) (Fig. 1). As a result of this topographic control, the W–E precipitation gradients  
45 are typically strongest in Scotland, and notably weaker across Ireland (Fig. 1B). Similarly, trends in  
46 mean annual air temperature are largely determined by topography, with notable altitudinal cooling  
47 (Fig. 1C). There is also a general cooling with latitude (Fig. 1C), but this latitudinal cooling is often  
48 difficult to differentiate from the control exerted by topography.

49 Though these climatic patterns currently prevail, the position, stability and strength of the PFJS  
50 vary not only seasonally and annually, but over much longer time periods (centuries to millennia). This  
51 variability is linked to North Atlantic sea surface temperatures, sea-ice extent, thermohaline circulation,  
52 and the extent of glaciation over North America and NW Europe (McManus et al., 1999). As such,  
53 synoptic climate patterns over Britain and Ireland are subject to change over multiple timescales. This  
54 is likely to have been particularly true during former periods of glaciation, when the growth of glaciers,  
55 and the expansion of sea-ice had a dramatic impact on North Atlantic climate (Renssen and Isarin, 1997;  
56 Renssen and Vandenberghe, 2003; Golledge et al., 2010). During the Younger Dryas Stadial (c. 12.9–

57 11.7 ka), for example, when much of Britain and Ireland experienced mountain and ice cap glaciation,  
58 it has been suggested that the southward displacement of the PFJS and associated increase in NE  
59 Atlantic sea-ice extent, resulted in accumulation season (winter) aridity in NW Europe (Renssen and  
60 Isarin, 1998; Renssen and Vandenberghe, 2003; Golledge et al., 2010).

61 While glacial deposits (e.g., landforms and sediments) are useful for inferring full glacial  
62 conditions, less is known about conditions during smaller scale glaciations, partly because relevant  
63 evidence is commonly removed by subsequent, more extensive, glacial advances (Kirkbride and  
64 Winkler, 2012). In Britain and Ireland, this is particularly true of evidence relating to periods prior to  
65 the local Last Glacial Maximum (LGM, c. 27 ka), when much of the region was occupied by the British-  
66 Irish Ice Sheet (BIIS) (Clark et al., 2012). Fortunately, the altitude and aspect of glacial cirques  
67 (hereafter 'cirques'), armchair-shaped hollows formed by the erosive action of mountain glaciers (Fig.  
68 2), are a potential source of this information, since their distribution is largely determined by climatic  
69 patterns during periods of glacier initiation (Barr and Spagnolo, 2015a), while their dimensions  
70 (including their depth) are largely determined by glacial erosion over tens of thousands of years (often  
71 continued in successive glacial cycles), which is likely maximised during the onset and termination of  
72 periods of glaciation (Crest et al., 2017). To make use of this potential, we map cirques across Britain  
73 and Ireland, and analyse their distribution (altitude and aspect) to obtain information about climate  
74 patterns during periods of mountain glaciation (when occupied by small glaciers). We do not conduct  
75 detailed analysis of cirque morphometry (size and shape), though these data are presented in Clark et  
76 al. (in press). Many of these cirques have been mapped previously (Table 1), but most studies were  
77 conducted prior to the widespread development and implementation of remote sensing and geographical  
78 information system (GIS) based techniques (e.g., Federici and Spagnolo, 2004; Spagnolo et al., 2017).  
79 This is therefore the first study to systematically map and analyse cirques across Britain and Ireland and  
80 to consider their regional palaeoclimatic implications.

81

## 82 **2. Methods**

### 83 **2.1. Cirque identification and mapping**

84 Cirques (defined according to Evans and Cox, 1974) were mapped from Bing Maps aerial  
85 imagery, Google Earth, and three digital elevation models (DEMs): SRTM (horizontal resolution ~30  
86 m, vertical accuracy ~16 m), ASTER GDEM (horizontal resolution 30 m, vertical accuracy ~17 m),  
87 and NEXTMap Great Britain™ (horizontal resolution 5 m, vertical accuracy ~0.5 m). Each of these  
88 sources was used to map or visualise every cirque, with the exception of the NEXTMap DEM, which  
89 was not used in Ireland (due to lack of coverage). Cirques were identified as large hollows, occupying  
90 valley-head or valley-side settings, bounded upslope by arcuate (in plan) headwalls but open down-  
91 valley (Fig. 2). Cirque headwalls curve around floors which slope more gently than the surrounding  
92 topography. Cirque lower limits are often marked by convex breaks-of-slope, referred to as a  
93 ‘thresholds’ (Evans and Cox, 1995), sometimes occupied by frontal moraines, marking the transition  
94 from shallow cirque floors to steeper topography below. Where thresholds were lacking, lower limits  
95 were drawn to coincide with the extent of cirque lateral spurs (Evans and Cox, 1995; Barr and Spagnolo,  
96 2015a).

97 Though an attempt was made to map all cirques, some subtle examples will undoubtedly be  
98 missing from the database. These cirques may resemble mass movement scars, or be difficult to identify  
99 from the remotely-sensed sources used here. In addition, there are situations where features of non-  
100 glacial origin (e.g., nivation hollows) will have been erroneously included in the database. To minimise  
101 such errors, much of the mapping was validated through comparison with published sources (Table 1).

102

## 103 **2.2. Cirque metrics and attributes**

104 For each cirque, metrics were calculated using the Automated Cirque Metric Extraction  
105 (ACME) GIS tool of Spagnolo et al. (2017). For the purposes of this investigation, we focus on cirque  
106 minimum altitude ( $Z_{\min}$ ) and mean aspect. Metric calculations are based on the SRTM DEM, since these  
107 data provide coverage for the entire cirque dataset. In order to validate the use of this DEM, metrics for  
108 cirques in Britain were also calculated using the ASTER GDEM and NEXTMap Great Britain™  
109 (Ireland was excluded because of lack of NEXTMap data). Analysis of variance revealed no significant  
110 differences between results from the three DEMs ( $p = 0.869$  for  $Z_{\min}$  and 0.503 for aspect).

111 In order to understand controls on cirque altitudes, and to assess the degree to which patterns  
112 in  $Z_{\min}$  reflect palaeoclimatic conditions, relationships between  $Z_{\min}$  and aspect were analysed, as were  
113 relationships between  $Z_{\min}$  and a number of cirque attributes. This approach of analysing statistical  
114 relationships between cirque altitudes, aspect and attributes has been used previously to analyse the  
115 palaeoclimatic implications of cirque populations elsewhere (Principato and Lee, 2014; Barr and  
116 Spagnolo, 2015b). In the present study, the attributes recorded for each cirque include location  
117 (coordinates), given by northing and easting, in km (measured from the centre point of each cirque, and  
118 recorded as OS British National Grid coordinates, extended to cover Ireland); the shortest distance from  
119 each cirque centre point to the modern coastline (in kilometres, calculated using the ArcGIS Euclidean  
120 distance tool); the shortest distance from each cirque centre point to the coastline directly to its west  
121 ( $270^{\circ}\text{N}$ ). Cirque northing is measured on the assumption that it represents a very general proxy for  
122 spatial patterns in temperature, while easting, and distance from the coastline are likely to reflect general  
123 proxies for patterns in precipitation (in this region dominated by North Atlantic westerlies). In addition,  
124 the dominant bedrock lithology of each cirque (i.e., the geological unit which accounts for the greatest  
125 surface area) was recorded. Information about bedrock lithology was based on GIS data from the British  
126 Geological Survey 1:625,000 scale Digital Geological Map of Great Britain (DiGMapGB-625, v.50,  
127 downloaded from the BGS) (2016) and the Geological Survey Ireland (McConnell and Gatley, 2006)  
128 1:500,000 bedrock geology map of Ireland (downloaded from the GSI). To simplify the analysis, 34  
129 geological units were categorised into 7 broader classes (Fig. 3).

130

131

### 132 **3. Results**

#### 133 **3.1. Cirque distribution**

134 A total of 2208 cirques were identified and mapped throughout the mountains of Scotland ( $n =$   
135 1139), Wales ( $n = 260$ ), Northern England ( $n = 172$ ) (plus one cirque in Exmoor), and around the  
136 periphery of Ireland ( $n = 637$ ) (Fig. 1D). Given the uneven distribution of cirques, it is worth noting  
137 that patterns for the entire database (discussed below) are largely determined by cirques in Ireland and

138 Scotland (~80% of the total dataset). The cirque database has been incorporated in the BRITICE version  
139 2 Glacial Map (Clark et al. in press) and is available for scrutiny or download from this source.

140

### 141 **3.2. Cirque altitudes**

142 Across the dataset,  $Z_{\min}$  ranges from 2 m to 1083 m, and shows notable spatial variability (Fig.  
143 1D).  $Z_{\min}$  shows statistically significant ( $p < 0.01$ ) rises from west to east, south to north, and with  
144 distance from the modern coastline (Fig. 4, Table 2). There is also a statistically significant relationship  
145 between  $Z_{\min}$  and mean aspect, with Fourier (harmonic) regression (Evans and Cox, 2005) revealing  
146 that  $Z_{\min}$  for WSW ( $259^\circ$ ) facing cirques is typically 71 m lower than those facing ENE ( $079^\circ$ ) (Table  
147 2). Multiple regression for easting, northing, and distance to the coastline (Table 2) reveals that, for the  
148 entire dataset, the attribute most closely related to  $Z_{\min}$  is distance to the coastline ( $t$ -value = 18.91),  
149 followed by northing ( $t$ -value = 15.91), then easting ( $t$ -value = 10.29). The regression is not significantly  
150 improved by inclusion of aspect.

151 When sub-populations are considered independently, only cirques in Scotland and Wales show  
152 statistically significant relationships between  $Z_{\min}$  and northing—with the former showing a northward  
153 rise then strong decline in  $Z_{\min}$ , and the latter showing a weak, but statistically significant, northward  
154 rise (Fig. 4A, Table 2). Cirques in Scotland and Ireland show statistically significant rises in  $Z_{\min}$  from  
155 west to east, and with distance from the modern coastline (Fig. 4, Table 2). The eastward rise in the  
156 altitudes of Scottish cirques was also illustrated and discussed by Linton (1959). Only cirques in  
157 Scotland show a statistically significant relationship between  $Z_{\min}$  and mean aspect, with  $Z_{\min}$  for WNW  
158 ( $284^\circ$ ) facing cirques typically 65 m lower than for those facing ESE ( $104^\circ$ ). Multiple regression reveals  
159 that for Scotland, the attribute most closely related to  $Z_{\min}$  is distance to the coastline ( $t$ -value = 7.66),  
160 followed by easting ( $t$ -value = 5.97); for Ireland, the attribute most closely related to  $Z_{\min}$  is easting ( $t$ -  
161 value = 8.26), followed by distance to the coastline ( $t$ -value = 5.43); and for Wales, the northward  
162 increase in  $Z_{\min}$  is the only statistically significant relationship (Table 2). The English cirques, excluding  
163 Exmoor, are narrowly clustered in space and do not show significant relationships.

164 When the shortest distance from each cirque centre point to the closest coastline directly to its  
165 west is considered,  $Z_{\min}$  for the entire dataset shows a statistically significant rise then decline with

166 increasing distance (Fig. 4D). The rise in  $Z_{\min}$  is seen in both Scotland and Ireland, but the subsequent  
167 decline is only seen in Ireland, and is largely controlled by comparatively low altitude cirques in eastern  
168 Ireland (i.e., in the Mourne and Wicklow Mountains), although comparatively low altitude cirques are  
169 also found in south-central Ireland and South Wales (Fig. 4D).

170

### 171 **3.3. Cirque aspect**

172 The entire cirque dataset shows a strong NE bias in aspect, with a population vector mean of  
173  $048.8^\circ$  (Fig. 5). This NE bias is evident (with some variation) across the study area (Fig. 5), and is  
174 observed for cirques in many other parts of the Northern Hemisphere (Evans, 1977). The entire dataset  
175 has an aspect vector strength (VS, which highlights the extent of deviation from a uniform distribution  
176 with aspect—see Evans, 1977) of 47% (Fig. 5). This is central to the range of results from 59 globally-  
177 distributed studies of cirque aspect summarised by Barr and Spagnolo (2015a) (table 4 in their paper),  
178 where vector strength (excluding studies from Britain and Ireland) ranges from 18 to 91%, with a mean  
179 value of 54%. Cirque sub-populations in central and eastern Scotland, Wales and England have vector  
180 strengths (46–59%) which are similar to this (biased) ‘global’ mean, whilst the vector strength of cirques  
181 in Ireland and the islands of western Scotland are notably lower (30–37%) (Fig. 5). Thus, vector strength  
182 generally increases from west to east (Fig. 5). Lower aspect vector strengths along the Atlantic coast  
183 indicate that cirques in these areas have a greater tendency to face varied directions. For example, by  
184 quadrant, Irish cirques account for 50% of the SW-facing total ( $n = 142$ ), but only 23% of NE-facing  
185 total ( $n = 1073$ ) (Table 3).

186 When cirques are grouped by  $Z_{\min}$ , a general altitudinal increase in population vector strength  
187 is evident (Fig. 6). This likely reflects spatial variability in both cirque aspect and altitude (with low  
188 vector strength and low  $Z_{\min}$  in coastal populations, and high vector strength and high  $Z_{\min}$  in interior  
189 regions). In other populations globally, cirques typically show an altitudinal decrease in vector strength  
190 (i.e., the opposite of the trend seen here), as marginal glacial conditions at low altitudes largely restrict  
191 glacier formation to poleward-facing slopes (resulting in high vector strength), whilst cooler  
192 temperatures at high altitudes allow glaciers to form on a range of slopes (resulting in low vector  
193 strength) (Olyphant, 1977; Barr and Spagnolo, 2013).

194

### 195 **3.4. Cirque geology**

196 One-way analysis of variance (ANOVA) was used to estimate the variability in  $Z_{\min}$  accounted  
197 for by different geological classes. These data indicate a statistically significant relationship between  
198  $Z_{\min}$  and geology (F-ratio = 97.7, F-crit = 2.1), though this is weakened (F-ratio = 8.9, F-crit = 2.1) when  
199 detrended for the influence of northing, easting, and distance from the modern coastline (using the  
200 regression equation from Table 2).

201

## 202 **4. Discussion**

203 The cirque record presented here indicates former sites of mountain glaciation in Britain and  
204 Ireland. However, it is not possible to establish when glaciers first generated each cirque, not how long  
205 they were ice-occupied, and this likely varied across the dataset (by region and altitude). Thus, the  
206 record represents a time-integrated pattern of conditions during periods of mountain glaciation (likely  
207 spanning multiple Quaternary glaciations). With this in mind, here we assess evidence for climatic and  
208 non-climatic controls on the altitude and aspect of cirques in Britain and Ireland, before considering the  
209 palaeoclimatic implications of the record.

210

### 211 **4.1. Climatic controls**

212 Based on cirque distribution (Fig. 1D), it is clear that air temperature (Fig. 1C) was an important  
213 control on former sites of mountain glaciation in Britain and Ireland—with glaciation favoured in the  
214 highest mountains, where temperatures are lowest (Fig. 1C and D). However, patterns in  $Z_{\min}$  and cirque  
215 aspect indicate that exposure to moisture from the North Atlantic was also a key control. For example,  
216 in Scotland and Ireland the strongest trends in  $Z_{\min}$  are the rise from west to east; with distance from the  
217 coastline; and with distance from the closest coastline directly to the west (Fig. 4). Scotland and Ireland  
218 thus fit a pattern found in other regions globally, where the altitudes of former mountain glaciers  
219 (indicated by cirques) increases with distance from a dominant moisture source (Peterson and Robinson,  
220 1969; Hassinen, 1998; Principato and Lee, 2014; Barr and Spagnolo, 2015b). This pattern is thought to  
221 reflect restricted precipitation in interior (non-coastal) regions, which confines mountain glaciers (and

222 cirque formation) to higher altitudes, where cooler temperatures limit melt and thereby compensate for  
223 reduced accumulation. At first glance, eastern Ireland (i.e., the Mourne and Wicklow Mountains) and,  
224 to a lesser degree, south-central Ireland and South Wales appear to be an exception to this, as cirque  
225 altitudes are generally low, given their distant location from the closest coastline directly to the west  
226 (Fig. 4D). This may reflect the comparatively weak orographic precipitation gradient in Ireland (Fig.  
227 1B), combined with the influence of moisture from the southwest.

228 Cirque aspect data (Fig. 5) reveal that former mountain glaciation was promoted on NE-facing  
229 slopes, where direct solar radiation is minimised (limiting melt). However, in coastal areas (i.e., in  
230 Ireland, and the islands of western Scotland), comparatively low vector strengths (Fig. 5) appear to  
231 indicate that variations in direct solar radiation were less important, and that mountain glaciers were  
232 able to occupy, and thereby form cirques on, other slopes, albeit in smaller numbers. In regions further  
233 from the Atlantic coastline, vector strengths are higher, and there is a notable N/NE/E bias in vector  
234 means (Fig. 5). The strong bias in these regions suggests that variations in direct solar radiation (i.e.,  
235 controls on ablation) were the dominant control on glacier aspect, with mountain glacier development  
236 promoted on north-facing slopes, where direct solar radiation is lowest, and on NE-facing slopes, which  
237 receive much of their direct solar radiation in the morning, when air temperatures are relatively low  
238 (Evans, 1977, 2006). The eastward bias, particularly evident in areas such as NW Wales (Fig. 5),  
239 potentially indicates that away from the North Atlantic, westerlies were more important in the  
240 redistribution of snow, thereby promoting the formation of mountain glaciers on leeward (east-facing)  
241 slopes, as well as acting as a source of direct precipitation. This implies that North Atlantic westerlies,  
242 though still important in regulating sites of glacier development, were comparatively moisture-starved  
243 by the time they reached such areas—implying a notable W–E precipitation gradient. In addition, cirque  
244 aspect shows a tendency somewhat more eastward of NE at higher altitudes, where lower temperatures  
245 and drier snow likely facilitated redistribution by wind (Fig. 5).

246 In eastern and south-central Ireland, there is considerable variability in cirque aspect (VS =  
247 34%, Fig. 5). Again, this likely reflects the comparatively weak precipitation gradients across Ireland,  
248 combined with the influence of moisture from the southwest. Similarly, in South Wales, the strong  
249 E/NE aspect bias in cirque aspect (VS = 69%, Fig. 5) may reflect the role of southwesterlies in

250 promoting glaciation on leeward (NE-facing) slopes (though it is difficult to differentiate between this  
251 potential control and the role of direct solar radiation in promoting glacier formation on these slopes).  
252 A broad distribution of aspects may also relate to the greater cloudiness of maritime climates.

253

#### 254 **4.2. Non-climatic controls**

255 Despite potential climatic controls on cirque altitude and aspect (Section 4.1.), non-climatic  
256 factors also need to be considered (Barr and Spagnolo, 2015a).

257 The first factor considered is topography, since high- and low-altitude mountain glaciers can  
258 only form, and thereby generate cirques, where high- and low-altitude topography (respectively) exist.  
259 Thus, the inland increase in  $Z_{\min}$  across Britain and Ireland (Fig. 4C), might, at least partly, reflect a  
260 corresponding increase in topography (Peterson and Robinson, 1969; Hassinen, 1998). To assess this  
261 potential, we compare  $Z_{\min}$  to the minimum and maximum altitudes within a 5 km radius of each cirque,  
262 and plot values relative to distance from the modern coastline (Fig. 4C), on the assumption that these  
263 data reflect regional trends in topography. Minimum altitudes show a general inland rise, but maximum  
264 altitudes show no clear inland trend, and topography often extends well above  $Z_{\min}$  (Fig. 4C). There is,  
265 therefore, little evidence to suggest that topography exerts a strong control on cirque altitudes, and is  
266 not considered to fully account for observed trends in  $Z_{\min}$ .

267 The second factor to consider is geology, which has the potential to exert control on both cirque altitude  
268 and aspect (Battey, 1960; Mîndrescu and Evans, 2014). For example, the relationships between  $Z_{\min}$   
269 and lithology (noted in Section 3.4.) might indicate a geological control on cirque altitudes. However,  
270 since this relationship is comparatively weak, when detrended for the influence of northing, easting,  
271 and distance from the modern coastline, it is not considered a dominant factor regulating  $Z_{\min}$  across the  
272 dataset. It is also probable that this relationship reflects spatial variability in both  $Z_{\min}$  and lithology. For  
273 example, in the mountains of central and eastern Scotland, where  $Z_{\min}$  is comparatively high, cirque  
274 lithology is dominated by Psammite or Pelite, whereas Granite or Gneiss cirques are typically found in  
275 lower altitude, coastal locations (Fig. 3). It is also possible that geological structure (i.e., the alignment  
276 of mountain ranges) exerts control on cirque aspect by regulating the orientation of slopes available for  
277 glacier development (Gordon, 2001; Evans, 2006; Bathrellos et al., 2014). However, as ridges in each

278 sub-region have a broad range of orientations, structural controls are likely local and are not considered  
279 to affect the aspect statistics cited here.

280         The third factor considered here is the role of post-glacial uplift and subsidence and their  
281 potential to displace cirques from the altitudes at which they were formed. This influence is most  
282 important in tectonically active areas (Bathrellos et al., 2014), and, fortunately, both Britain and Ireland  
283 have been tectonically stable during the Quaternary. However, glacial isostatic adjustment has occurred,  
284 and its extent has been spatially and temporally variable (Bradley et al., 2011; Kuchar et al., 2012). Of  
285 potential note for this study is the disparity between SW Ireland, where isostasy currently results in  
286 subsidence rates of  $\sim 0.5 \text{ mm a}^{-1}$ , and central Scotland, where uplift is occurring at  $\sim 1.5 \text{ mm a}^{-1}$  (Shennan  
287 et al., 2009). Assuming that glacier initiation occurred on a land surface unaffected by glacial loading,  
288 this spatial variability is likely to have had some impact on trends in  $Z_{\min}$ . However,  $Z_{\min}$  also varies  
289 even over comparatively small spatial scales (e.g., in western Scotland), where differences in uplift are  
290 likely modest. Also, cirques in central Scotland (where glacial isostatic depression was greatest) are  
291 presumably still depressed below the altitudes at which they formed, while cirques in SW Ireland (where  
292 subsidence is currently occurring) are presumably elevated above the altitudes at which they formed.  
293 Thus, if cirque altitudes were corrected for residual glacial isostatic adjustment, this would strengthen  
294 the general SW–NE  $Z_{\min}$  gradient currently observed.

295         The final factor to be considered here is the possibility that trends in  $Z_{\min}$ , at least partly, reflect  
296 spatial variability in the extent of cirque deepening. This is based on the premise that  $Z_{\min}$  is controlled  
297 not only by the altitudes at which former glaciers initiated, but also by the extent to which these glaciers  
298 eroded vertically. For example, given that documented cirque floor erosion rates range from  $\sim 0.076$   
299  $\text{mm yr}^{-1}$  to  $5.9 \text{ mm yr}^{-1}$  (Barr and Spagnolo, 2015a), over 100,000 years of glacial occupation this would  
300 result in a  $\sim 580 \text{ m}$  difference in depth between a heavily and minimally eroded cirque. This would be  
301 sufficient to account for some  $Z_{\min}$  trends across Britain and Ireland. To test this possibility, here we  
302 analyse trends in cirque depth ( $H$ ) (i.e., maximum – minimum altitudes, see Spagnolo et al., 2017), and  
303 make comparisons with trends in  $Z_{\min}$ .

304         When the entire dataset is considered,  $H$  shows a significant reduction from north to south, and  
305 with distance from the modern coastline (Fig. 7). However, these relationships are not strong (typically,

306  $R^2 = 0.03\text{--}0.08$ , Table 4), and the southward reduction in H (Fig. 7A), fails to explain the corresponding  
307 decline in  $Z_{\min}$  (Fig. 4A). In Wales, relationships are stronger ( $R^2 = 0.08\text{--}0.21$ , Table 4), but, again, the  
308 dominant pattern is a southward reduction in H (Fig. 7A), which fails to explain the corresponding  
309 decline in  $Z_{\min}$  (Fig. 4A).

310         Given the above, spatial trends in H are not considered to fully account for trends in  $Z_{\min}$ .  
311 However, the consistent pattern of increasing H with proximity to the coastline (Fig. 7C and D) might  
312 indicate that moisture availability in these areas not only promoted the initiation of comparatively low  
313 altitude glaciers, but may also have resulted in glaciers that were comparatively efficient at cirque  
314 deepening. Cirque deepening is often thought to be promoted by long-lasting (and/or repeated)  
315 occupation by cirque-type glaciers (i.e., small glaciers confined to their cirques), and/or occupation by  
316 particularly dynamic glaciers (Bathrellos et al., 2014; Barr and Spagnolo, 2015a). Thus, the increase in  
317 H with proximity to the coastline might indicate that, during glacial cycles, cirques in these locations  
318 were occupied by comparatively small glaciers (often confined to their cirques). This might reflect  
319 marginal glacial conditions in these climatically less favourable (in terms of solar radiation) low-altitude  
320 locations. By contrast, in regions such as central Scotland, cirques may have readily become occupied  
321 by large (non cirque-type) glaciers (Golledge et al., 2008), which are often considered inefficient at  
322 cirque deepening (Barr and Spagnolo, 2013). In addition, glaciers in coastal locations may have been  
323 comparatively dynamic, with greater mass turnover and greater basal velocities than elsewhere, since  
324 they occupied comparatively maritime climatic conditions. Thus, cirque depth data might indicate that,  
325 during glacial cycles, cirques in coastal locations were more often occupied by dynamic and/or cirque-  
326 type glaciers, while larger and/or less dynamic glaciers dominated further inland.

327

### 328 **4.3. Palaeoclimatic inferences**

329         We suggest that patterns in cirque altitude and aspect across Britain and Ireland are not  
330 controlled by variations in topography, geology or glacial isostasy, but largely reflect climatic  
331 conditions during former periods of mountain glaciation, and are perhaps enhanced (in places) by  
332 regional differences in the extent of cirque deepening. On this basis, the cirque record appears to  
333 indicate that during periods of mountain glaciation, moisture supply across Britain and Ireland was

334 dominated by westerlies. The data suggest that during such periods precipitation patterns very similar  
335 to present, with a general W–E gradient (strongest in Western Scotland), a S–N gradient in Wales, and  
336 a more complex picture in eastern and South-Central Ireland. In addition, cirque depth data potentially  
337 indicate former maritime conditions in coastal locations (promoting dynamic glaciation and cirque  
338 deepening), with more continental conditions further inland (resulting in less dynamic glaciation and  
339 limited cirque deepening)

340

## 341 **5. Conclusions**

342 In this study, glacial cirques are mapped and their altitudes and aspect analysed. These attributes  
343 provide information about climate patterns during former periods of mountain glaciation in Britain and  
344 Ireland. The main study findings are summarised as follows:

- 345 1. Cirque altitude and aspect indicate that although air temperatures were important, exposure  
346 to moisture-bearing air masses was the key factor in regulating sites of former mountain  
347 glaciation in Britain and Ireland (as would be expected in a maritime environment). Non-  
348 climatic factors (including topography, geology, and isostasy) are also likely to have had  
349 an impact, but do not explain region-wide patterns.
- 350 2. The record indicates that climatic patterns in Britain and Ireland were similar to present,  
351 with moisture largely derived from North Atlantic westerlies, resulting in a notable W–E  
352 precipitation gradient, which was strongest in western Scotland.
- 353 3. Trends in cirque altitude may also reflect regional differences in the extent of cirque  
354 deepening—largely controlled by the dimensions and dynamics of the glaciers that came  
355 to occupy them (likely during multiple Quaternary glaciations). Specifically, comparatively  
356 deep cirques in coastal locations may reflect the former presence of dynamic and/or cirque-  
357 type glaciers (occupying a maritime climate), while less-deep cirques further inland may  
358 reflect the former presence of larger and/or less dynamic ice masses (occupying more  
359 continental conditions).

360

## 361 **Acknowledgements.**

362 We thank Magali Delmas and an anonymous reviewer for their corrections, comments and suggestions.

363 We are also grateful to the editor Paul Hesse.

364

365

## 366 **References**

367

368 Ballantyne, C.K., 2007a. The Loch Lomond Readvance on north Arran, Scotland: glacier reconstruction  
369 and palaeoclimatic implications. *Journal of Quaternary Science* 22 (4), 343-359.

370

371 Ballantyne, C.K., 2007b. Loch Lomond Stadial glaciers in North Harris, Outer Hebrides, north-west  
372 Scotland: glacier reconstruction and palaeoclimatic implications. *Quaternary Science Reviews* 26 (25),  
373 3134-3149.

374

375 Bathrellos, G.D., Skilodimou, H.D., Maroukian, H., 2014. The Spatial Distribution of Middle and Late  
376 Pleistocene Cirques in Greece. *Geogr. Ann. Ser. A Phys. Geogr.* 96 (3), 323–338.

377

378 Battey, M.H., 1960. Geological factors in the development of Veslgjuv-Botn and Vesl-Skautbotn. In:  
379 Lewis, W.V. (Ed.), *Norwegian Cirque Glaciers*. Royal Geographical Society Research Series 4, 5–10.

380

381 Barr, I.D., Spagnolo, M., 2013. Palaeoglacial and palaeoclimatic conditions in the NW Pacific, as  
382 revealed by a morphometric analysis of cirques upon the Kamchatka Peninsula. *Geomorphology* 192,  
383 15–29.

384

385 Barr, I.D., Spagnolo, M., 2015a. Glacial cirques as palaeoenvironmental indicators: Their potential and  
386 limitations. *Earth-Science Reviews* 151, 48–78.

387

388 Barr, I.D., Spagnolo, M., 2015b. Understanding controls on cirque floor altitudes: insights from  
389 Kamchatka. *Geomorphology* 248, 1–13.

390

391 Bradley, S.L., Milne, G.A., Shennan, I., Edwards, R., 2011. An improved glacial isostatic adjustment  
392 model for the British Isles. *Journal of Quaternary Science* 26 (5), 541–552.

393

394 Clark, C.D., Ely, J.C., Greenwood, S.L., Hughes, A.L.C., Meehan, R., Barr, I.D., Bateman, M.D.,  
395 Bradwell, T., Doole, J., Evans, D.J.A., Jordan, C., Monetys, X., Pellicer, X., Sheey, M., in press.  
396 BRITICE Glacial Map, version two: A map and GIS database of glacial landforms of the last British-  
397 Irish Ice Sheet. *Boreas*.

398

399 Clark, C.D., Hughes, A.L., Greenwood, S.L., Jordan, C., Sejrup, H.P., 2012. Pattern and timing of  
400 retreat of the last British-Irish Ice Sheet. *Quaternary Science Reviews* 44, 112–146.

401

402 Clough, R.M.K., 1974. *The Morphology and Evolution of the Lakeland Corries*. Unpublished M. Phil,  
403 dissertation in Geography, Queen Mary College, University of London, England.

404

405 Clough, R.M.K., 1977. Some aspects of corrie initiation and evolution in the English Lake District.  
406 *Proc. Cumb. Geol. Soc.* 3, 209–232

407

408 Crest, Y., Delmas, M., Braucher, R., Gunnell, Y., Calvet, M., ASTER Team, 2017. Cirques have growth  
409 spurts during deglacial and interglacial periods: Evidence from <sup>10</sup>Be and <sup>26</sup>Al nuclide inventories in the  
410 central and eastern Pyrenees. *Geomorphology* 278, 60–77.

411

412 Evans, I.S., 1977. World-Wide Variations in the Direction and Concentration of Cirque and Glacier  
413 Aspects. *Geogr. Ann. Ser. A Phys. Geogr.* 59 (3/4), 151–175.

414

415 Evans, I.S., 1999. Was the cirque glaciation of Wales time-transgressive, or not? *Ann. Glaciol.* 28, 33–  
416 39.

417

418 Evans, I.S., 2006. Local aspect asymmetry of mountain glaciation: a global survey of consistency of  
419 favoured directions for glacier numbers and altitudes. *Geomorphology* 73 (1), 166–184.  
420

421 Evans, I.S., Cox, N.J., 1974. Geomorphometry and the operational definition of cirques. *Area* 6, 150–  
422 153.  
423

424 Evans, I.S., Cox, N.J., 1995. The form of glacial cirques in the English Lake District, Cumbria. *Z.  
425 Geomorphol.* 39, 175–202.  
426

427 Evans, I.S., Cox, N.J., 2005. Global variations of local asymmetry in glacier altitude: separation of  
428 north–south and east–west components. *J. Glaciol.* 51, 469–482.  
429

430 Federici, P.R., Spagnolo, M., 2004. Morphometric analysis on the size, shape and areal distribution of  
431 glacial cirques in the Maritime Alps (Western French-Italian Alps). *Geogr. Ann. Ser. A Phys. Geogr.*  
432 86 (3), 235–248.  
433

434 Gолledge N.R., Hubbard, A.L., Bradwell, T., 2010. Influence of seasonality on glacier mass balance,  
435 and implications for palaeoclimate reconstructions. *Climate Dynamics* 35, 757–770.  
436

437 Gолledge, N.R., Hubbard, A., Sugden, D.E., 2008. High-resolution numerical simulation of Younger  
438 Dryas glaciation in Scotland. *Quaternary Science Reviews* 27 (9), 888–904.  
439

440 Godard, A., 1965. *Recherches de géomorphologie en Écosse du Nord-Ouest*. Les Belles Lettres, Paris.  
441

442 Gordon, J.E., 1977. Morphometry of cirques in the Kintail–Affric–Cannich area of northwest Scotland.  
443 *Geogr. Ann. Ser. A Phys. Geogr.* 59, 177–194.  
444

445 Gordon, J.E., 2001. The corries of the Cairngorm Mountains. *Scott. Geogr. Mag.* 117 (1), 49–62.

446

447 Harker, A., 1901. Ice erosion in the Cuillin Hills, Skye. *Trans. R. Soc. Edinb.* 40 (2), 221–252.

448

449 Hassinen, S., 1998. A morpho-statistical study of cirques and cirque glaciers in the Senja-Kilpisjärvi  
450 area, northern Scandinavia. *Norsk Geografisk Tidsskrift-Norwegian Journal of Geography* 52 (1), 27–  
451 36.

452

453 Hijmans, R.J., Cameron, S.E., Parra, J.L., Jones, P.G., Jarvis, A., 2005. Very high resolution  
454 interpolated climate surfaces for global land areas. *International journal of climatology*, 25(15),  
455 pp.1965-1978.

456

457 Hurrell, J.W., Deser, C., 2010. North Atlantic climate variability: the role of the North Atlantic  
458 Oscillation. *Journal of Marine Systems* 79 (3), 231–244.

459

460 Kirkbride, M.P. and Winkler, S., 2012. Correlation of Late Quaternary moraines: impact of climate  
461 variability, glacier response, and chronological resolution. *Quaternary Science Reviews* 46, 1–29.

462

463 Kuchar, J., Milne, G., Hubbard, A., Patton, H., Bradley, S., Shennan, I., Edwards, R., 2012. Evaluation  
464 of a numerical model of the British–Irish ice sheet using relative sea-level data: implications for the  
465 interpretation of trimline observations. *Journal of Quaternary Science* 27 (6), 597–605.

466

467 Lewis, C.A., 1970. The glaciation of the Brecknock Beacons. *Brycheiniog (The Brecknock Society)*  
468 14, 97–120.

469

470 Linton, D.L., 1959. Morphological contrasts of Eastern and Western Scotland. In: Miller, R., Watson,  
471 J.W., *Geographical essays in memory of Alan G. Ogilvie*. Thomas Nelson and Sons Ltd., London, 16–  
472 45.

473

474 Mayes, J., Wheeler, D., 2013. Regional weather and climates of the British Isles-Part 1:  
475 Introduction. *Weather* 68 (1), 3–8.  
476

477 McConnell, B., Gatley, S. (2006). Bedrock Geology map of Ireland. 1 to 500,000 scale. Geological  
478 Survey Ireland, Dublin.  
479

480 McManus, J.F., Oppo, D.W., Cullen, J.L., 1999. A 0.5-million-year record of millennial-scale climate  
481 variability in the North Atlantic. *Science* 283 (5404), 971–975.  
482

483 Mîndrescu, M., Evans, I.S., 2014. Cirque form and development in Romania: allometry and the buzzsaw  
484 hypothesis. *Geomorphology* 208, 117–136.  
485

486 Olyphant, G.A., 1977. Topoclimate and the depth of cirque erosion. *Geografiska Annaler. Series A.*  
487 *Physical Geography* 59 (3/4), 209–213.  
488

489 Pearce, D., 2014. Reconstructing Younger Dryas glaciation in the Tweedsmuir Hills, Southern Uplands,  
490 Scotland: Style, dynamics and palaeoclimatic implications, Unpublished PhD thesis, University of  
491 Worcester.  
492

493 Peterson, J.A., Robinson, G., 1969. Trend surface mapping of cirque floor levels. *Nature* 222, 75–76.  
494

495 Pippin, T., 1967. Comparative glacio-morphological research in Alpine, Hercynian and Caledonian  
496 mountains of Europe. In: Sporck, J.A. (Ed.), *Mdlangés de géographie offerts a M. Omer Tulippe*, Vol.  
497 1, Gembloux, Belgique, J. Duculot, pp. 87–104.  
498

499 Principato, S.M., Lee, J.F., 2014. GIS analysis of cirques on Vestfirðir, northwest Iceland: implications  
500 for palaeoclimate. *Boreas* 43, 807–817.  
501

502 Rea B.R., McCarron S., 2008. The Younger Dryas in the north of Ireland. In North of Ireland: Field  
503 Guide, Whitehouse NJ, Roe HM, McCarron S, Knight J (eds). Quaternary Research Association:  
504 London.

505

506 Renssen, H., Isarin, R.F.B., 1998. Surface temperature in NW Europe during the Younger Dryas:  
507 AGCM simulation compared with temperature reconstructions. *Climate Dynamics* 14, 33–44.

508

509 Renssen, H., Vandenberghe, J., 2003. Investigation of the relationship between permafrost distribution  
510 in NW Europe and extensive winter sea-ice cover in the North Atlantic Ocean during the cold phases  
511 of the Last Glaciation. *Quaternary Science Reviews* 22, 209–223.

512

513 Sale, C., 1970. Cirque Distribution in Great Britain: A Statistical Analysis of Variations in Elevation,  
514 Aspect and Density. Unpublished M.Sc. dissertation, Department of Geography, University College,  
515 London.

516

517 Seddon, B., 1957. The late-glacial cwm glaciers in Wales. *J. Glaciol.* 3, 94–99.

518

519 Shennan, I., Milne, G., Bradley, S., 2009. Late Holocene relative land-and sea-level changes: providing  
520 information for stakeholders. *GSA today* 19 (9), 52–53.

521

522 Sissons, J.B., 1967. The evolution of Scotland's scenery. Oliver and Boyd, Edinburgh.

523

524 Spagnolo, M., Pellitero, R., Barr, I.D., Ely, J.C., Pellicer, X.M., Rea, B.R., 2017. ACME, a GIS tool for  
525 Automated Cirque Metric Extraction. *Geomorphology* 278, 280–286.

526

527 Spencer, K., 1959. Corrie aspect in the English Lake District. Don. *Journal of the Sheffield University*  
528 *Geographical Society* 3, 6–9.

529

- 530 Sugden, D.E., 1969. The age and form of corries in the Cairngorms. *Scott. Geogr. Mag.* 85, 34–46.
- 531
- 532 Temple, P.H., 1965. Some aspects of cirque distribution in the west-central Lake District, northern
- 533 England. *Geogr. Ann. Ser. A Phys. Geogr.* 47, 185–193.
- 534
- 535 Unwin, D.J., 1973. The distribution and orientation of corries in northern Snowdonia, Wales. *Trans.*
- 536 *Inst. Br. Geogr.* 58, 85–97.

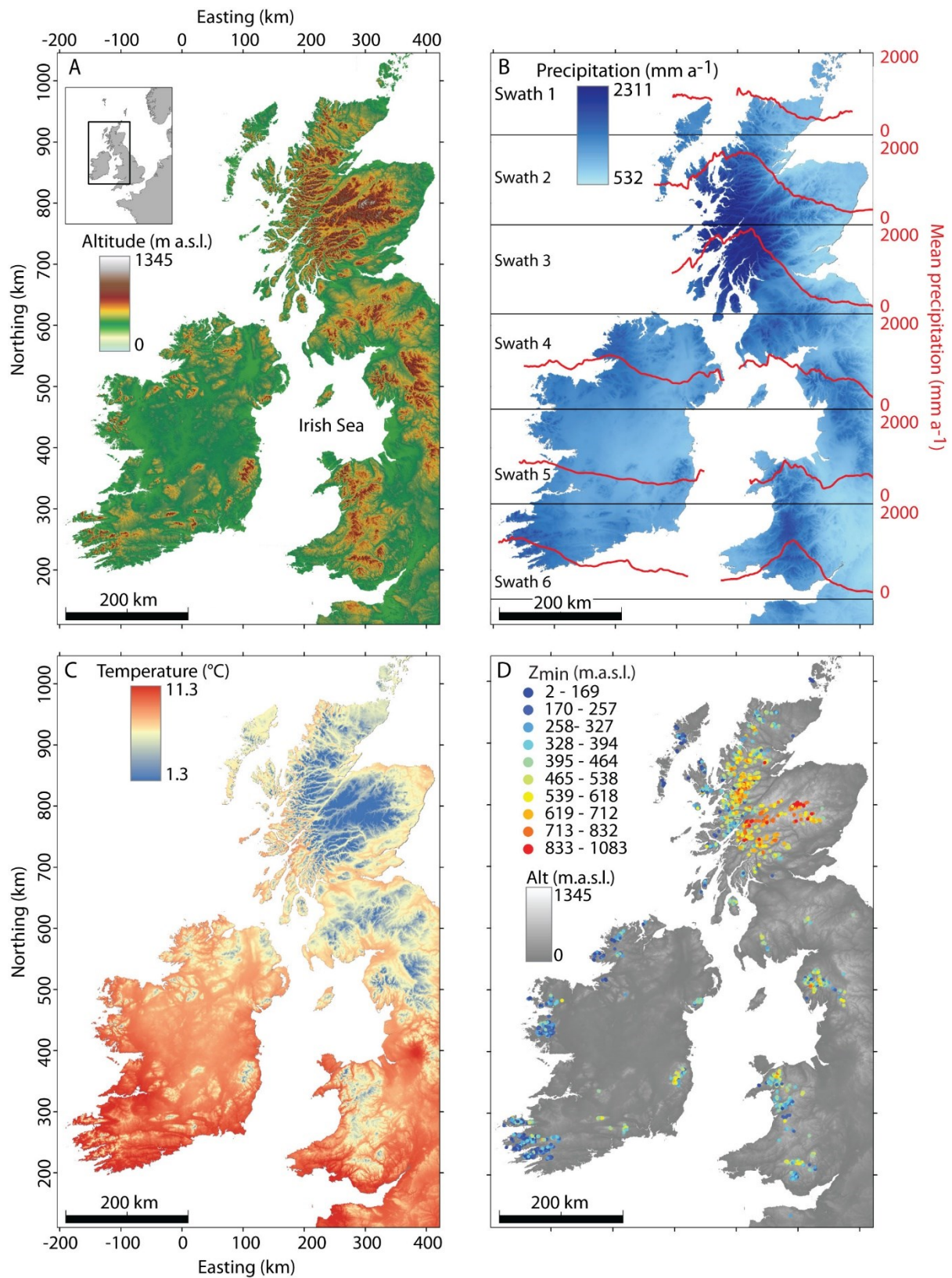
537

538

539

540

541



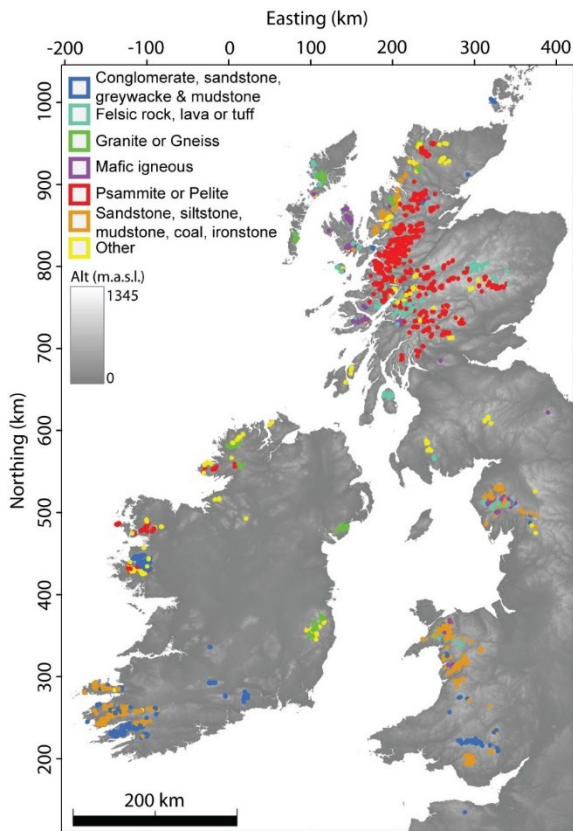
542

543 Fig. 1. Maps of the upland (cirque-occupied) regions of Britain and Ireland. (A) Topographic map  
 544 (shown using SRTM DEM data). (B) Gridded annual average precipitation, and (C) mean annual  
 545 temperature, for the 1950–2000 period (Hijmans et al., 2005). (D) Cirques (n = 2208), coloured

546 according to minimum altitude above sea level ( $Z_{\min}$ ). In (B), the red cross-sections show mean  
 547 precipitation values for the different swaths (values shown in red at the right side of the image).  
 548 Coordinates in this figure represent the OS British National Grid, extended to cover Ireland.  
 549

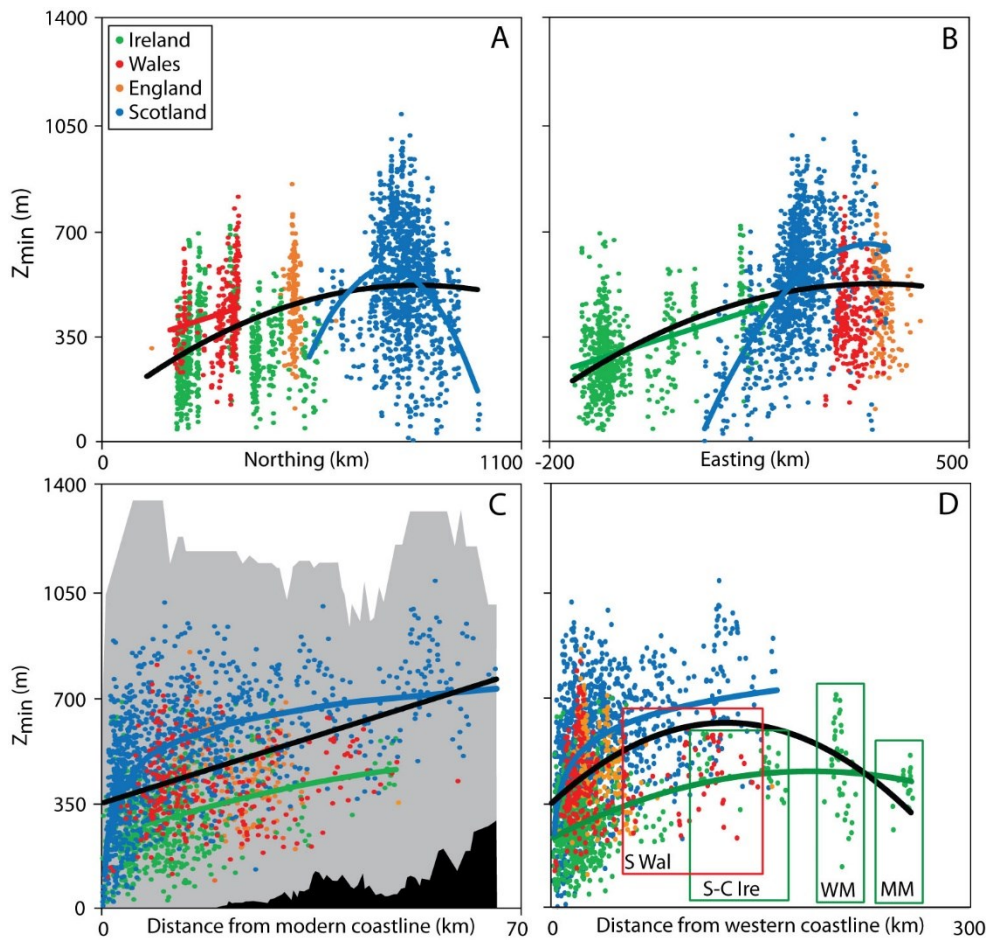


550  
 551 Fig. 2. Example cirque (Choire Dheirg, Scotland, 58.197°N, 4.974°W), mapped as a blue polygon, and  
 552 shown in getmapping™ aerial image, viewed obliquely in Google Earth™.  
 553



554

555 Fig 3. Cirques classified according to their dominant geological class.



556

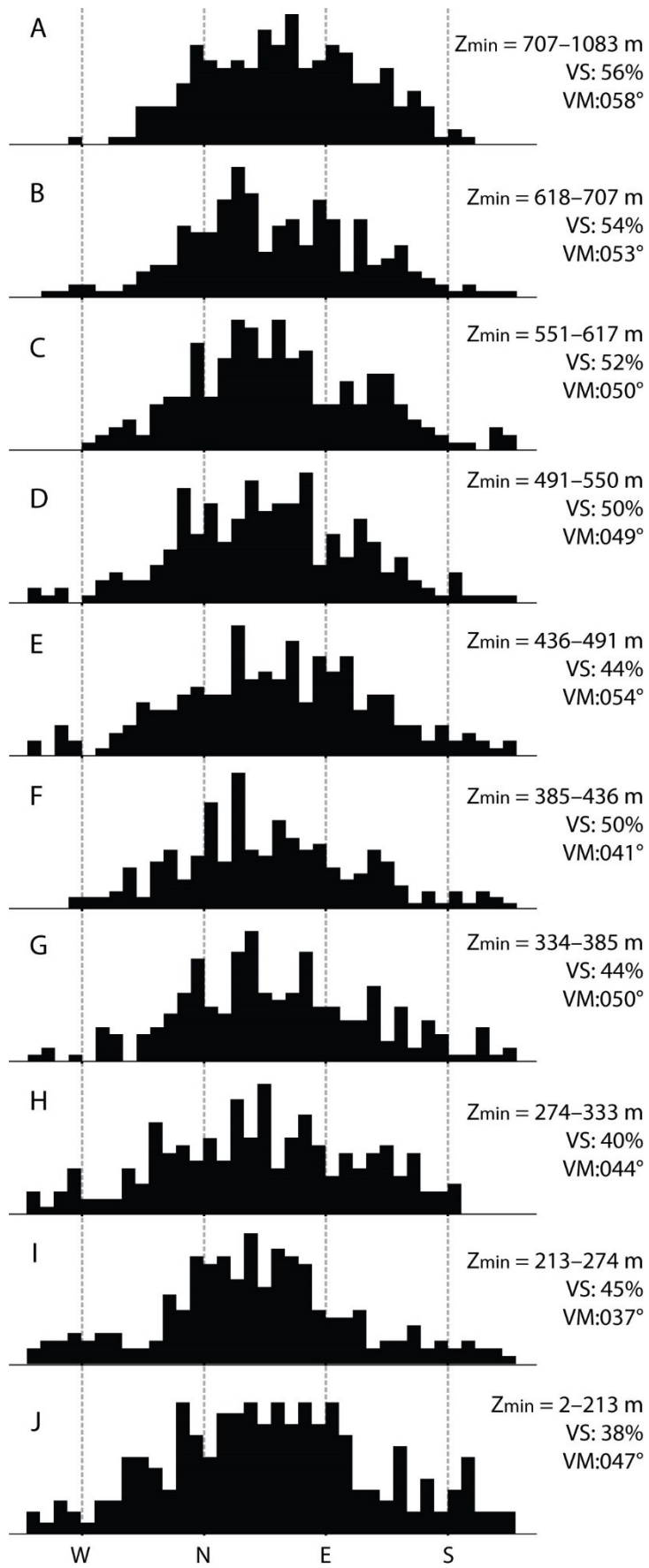
557

558 Fig. 4. Cirque minimum altitude ( $Z_{min}$ ) plotted against (A) northing; (B) easting; (C) distance from the  
 559 modern coastline; and (D) distance from the closest coastline directly to the west. In each case, the solid  
 560 black line reflects the regression line for the entire cirque dataset, whilst coloured lines reflect national  
 561 cirque populations (lines are only plotted where relationships are significant, i.e.,  $p < 0.01$ , see Table  
 562 2). In (C), the maximum (grey shaded area) and minimum (black shaded area) topography (based on  
 563 the region within a 5 km radius of each cirque) are also plotted. In (D), regions labelled in boxes are:  
 564 the Mourne Mountains (MM), Wicklow Mountains (WM), South-central Ireland (S-C Ire) and South  
 565 Wales (S Wales).

566

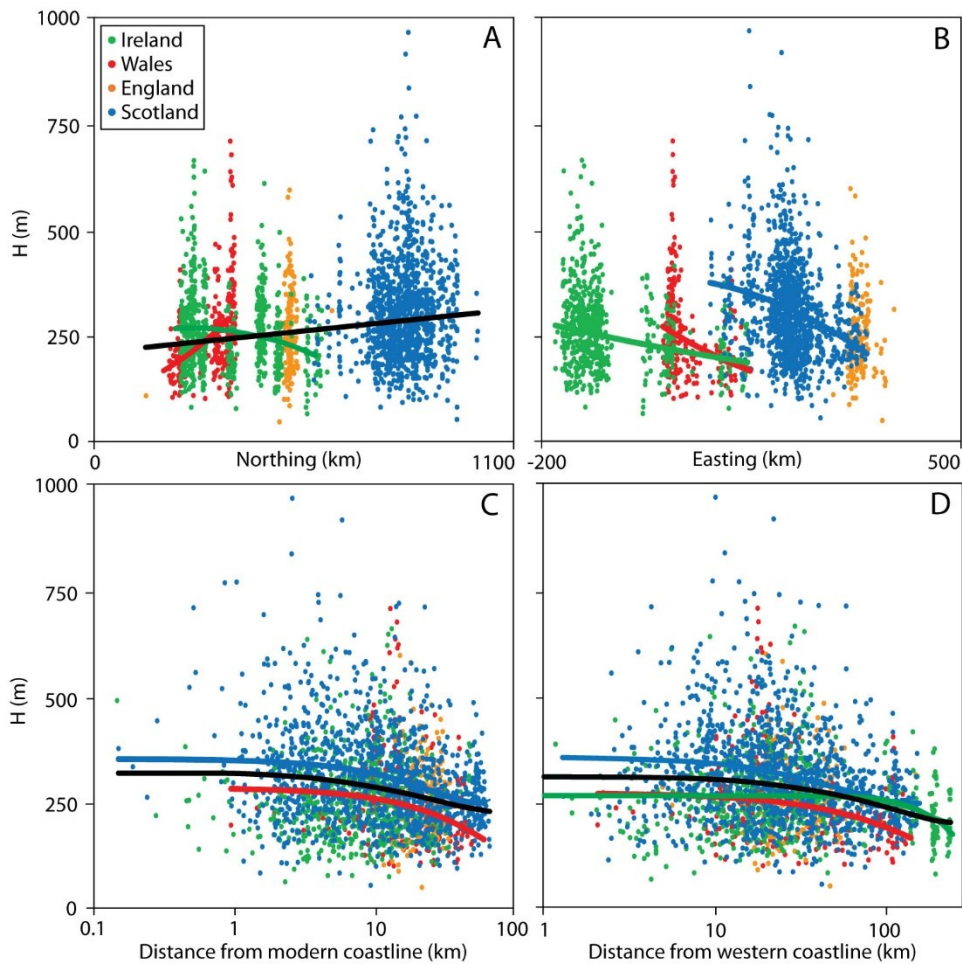


573 Ireland. For each population, the aspect vector mean (VM), vector strength (VS, which highlights the  
574 extent of deviation from a uniform distribution with aspect), and number of cirques (n) are recorded  
575  
576  
577  
578  
579



581 Fig. 6. Aspect histograms for cirque populations grouped according to  $Z_{\min}$  (221 cirques are represented  
 582 in each diagram, with the exception of (A) where 219 are represented). Groups range from (A) the  
 583 highest cirques, to (J) the lowest. For each group, the aspect vector strength (VS), vector mean (VM),  
 584 and range in  $Z_{\min}$  are recorded.

585



586

587 Fig. 7. Cirque depth (H) plotted against (A) northing; (B) easting; (C) distance from the modern  
 588 coastline; and (D) distance from the closest coastline directly to the west. In each case, the solid black  
 589 line reflects the regression line for the entire cirque dataset, whilst coloured lines reflect national cirque  
 590 populations (lines are only plotted where relationships are significant, i.e.,  $p < 0.01$ , see Table 4). Note:  
 591 in (C) and (D), the x-axes are plotted on logarithmic scales.

592

593

594

595 Table 1. Summary of previous investigations of cirques in Britain and Ireland.

| Citation            | Region                              | Number of cirques mapped |
|---------------------|-------------------------------------|--------------------------|
| Evans (2006)        | Wales                               | 260                      |
| Evans (1999)        | Wales                               | 228                      |
| Gordon (1977)       | Kintail-Aifric-Cannich, NW Scotland | 260                      |
| Clough (1974, 1977) | Cumbria, England                    | 198                      |
| Unwin (1973)        | Snowdonia, NW Wales                 | 81                       |
| Lewis (1970)        | Brecon Beacons, Wales               | 13                       |
| Sale (1970)         | Scotland                            | 876                      |
|                     | Cumbria, England                    | 104                      |
|                     | North Wales                         | 118                      |
|                     | South Wales                         | 15                       |
| Sugden (1969)       | Cairngorms, Scotland                | 30                       |
| Pippan (1967)       | Cumbria, England                    | 28                       |
| Sissons (1967)      | Scotland                            | 347                      |
| Godard (1965)       | NW Scotland                         | 437                      |
| Temple (1965)       | West-Central Cumbria, England       | 73                       |
| Spencer (1959)      | Cumbria, England                    | 67                       |
| Seddon (1957)       | Snowdonia, NW Wales                 | 34                       |
| Harker (1901)       | Cuillin, Scotland                   | 52                       |

596

597 Table 2. Regression of minimum altitude ( $Z_{\min}$ ) against northing (N), easting (E), distance from the  
 598 modern coastline (dist), and aspect ( $\theta$ ) for cirques across Britain and Ireland. Significant relationships  
 599 (i.e., where  $p < 0.01$ ) for N, E and dist are plotted in Fig. 3.

| Region              | Variable            | Equation   | p-value                                 | R <sup>2</sup> |
|---------------------|---------------------|--|---|----------------|
| Total               | Northing            | $Z_{\min} = -0.001N^2 + 0.998N + 93.65$  | <0.01                                   | 0.197          |
|                     | Easting             | $Z_{\min} = -0.001E^2 + 0.737E + 375.72$   | <0.01                                   | 0.271          |
|                     | Dist.               | $Z_{\min} = 6.552\text{dist} + 349.210$  | <0.01                                   | 0.205          |
|                     | Aspect              | $Z_{\min} = 6.791\cos\theta + 34.834\sin\theta + 434.79$   | <0.01                                   | 0.011          |
|                     | N, E, dist.         | $Z_{\min} = 0.246N + 0.264E + \mathbf{5.065}\text{dist} + 187.39$                                      | <0.01                                   | 0.403          |
|                     | N, E, dist., aspect | $Z_{\min} = 0.247N + 0.263E + \mathbf{5.049}\text{dist} - 5.699\cos\theta + 2.411\sin\theta + 188.11$  | <0.01                                   | 0.404          |
|                     | Scotland            | Northing   | $Z_{\min} = -0.007N^2 + 11.362N - 3782$ | <0.01          |
| Easting             |                     | $Z_{\min} = -0.013E^2 + 7.793E - 507.47$   | <0.01                                   | 0.310          |
| Dist.               |                     | $Z_{\min} = 101.57 \ln(\text{dist}) + 303.74$  | <0.01                                   | 0.339          |
| Aspect              |                     | $Z_{\min} = -7.745\cos\theta + 31.61\sin\theta + 524.19$   | <0.01                                   | 0.001          |
| N, E, dist.         |                     | $Z_{\min} = -0.133N + 1.048E + \mathbf{3.87}\text{dist} + 354.48$                                      | <0.01                                   | 0.295          |
| N, E, dist., aspect |                     | $Z_{\min} = -0.141N + 1.030E + \mathbf{3.86}\text{dist} - 2.416\cos\theta + 19.251\sin\theta + 358.13$ | <0.01                                   | 0.299          |
| Ireland             |                     | Northing   | Not stat. sig.                          | 0.588          |
|                     | Easting             | $Z_{\min} = 0.001E^2 + 0.651E + 344.01$  | <0.01                                   | 0.152          |
|                     | Dist.               | $Z_{\min} = -0.033\text{dist}^2 + 6.656\text{dist} + 240.36$   | <0.01                                   | 0.131          |
|                     | Aspect              | Not stat. sig.   | 0.739                                   | n/a            |
|                     | N, E, dist.         | $Z_{\min} = -0.149N + \mathbf{0.558}E + 3.21\text{dist} + 368.70$                                      | <0.01                                   | 0.215          |
| Wales               | Northing            | $Z_{\min} = 0.393N + 297.72$   | <0.01                                   | 0.031          |
|                     | Easting             | Not stat. sig.   | 0.733                                   | n/a            |
|                     | Dist.               | Not stat. sig.   | 0.157                                   | n/a            |
|                     | Aspect              | Not stat. sig.   | 0.243                                   | n/a            |
| England             | Northing            | Not stat. sig.   | 0.367                                   | n/a            |
|                     | Easting             | Not stat. sig.   | 0.023                                   | n/a            |
|                     | Dist.               | Not stat. sig.   | 0.182                                   | n/a            |
|                     | Aspect              | Not stat. sig.   | 0.130                                   | n/a            |

600 For equations based on multiple regression, the coefficient and variable with the strongest  $t$  value is in  
 601 **bold face**.

602  
603  
604

Table 3. Cirque frequency by quadrant, illustrating differences between Ireland and the rest of the cirque population.

|             | NE   | SE  | SW  | NW  | Total |
|-------------|------|-----|-----|-----|-------|
| Total       | 1072 | 535 | 142 | 459 | 2208  |
| Ireland     | 250  | 153 | 71  | 163 | 637   |
| Rest        | 822  | 382 | 71  | 296 | 1571  |
| Ireland (%) | 23   | 29  | 50  | 36  | 29    |

605  
606  
607  
608

Table 4. Regression of cirque depth (H) against northing (N), easting (E), distance from the modern coastline (dist), and distance from the closest coastline directly to the west (distW) for cirques across Britain and Ireland. Significant relationships (i.e., where  $p < 0.01$ ) are plotted in Fig. 6.

| Region   | Variable | Equation   | p-value | R <sup>2</sup> |
|----------|----------|--|---------|----------------|
| Total    | Northing | $H = 215.44e^{0.0003N}$                                | <0.01   | 0.049          |
|          | Easting  | Not stat. sig.   | 0.362   | n/a            |
|          | Dist.    | $H = 0.038\text{dist}^2 - 3.421\text{dist} + 319.63$   | <0.01   | 0.041          |
|          | DistW    | $H = 0.002\text{distW}^2 - 0.860\text{distW} + 311.09$ | <0.01   | 0.049          |
| Scotland | Northing | Not stat. sig.   | 0.120   | n/a            |
|          | Easting  | $H = -0.001E^2 - 0.062E + 386.17$                      | <0.01   | 0.068          |
|          | Dist.    | $H = 0.037\text{dist}^2 - 3.918\text{dist} + 352$      | <0.01   | 0.077          |
|          | DistW    | $H = 0.007\text{distW}^2 - 1.777\text{distW} + 354.64$ | <0.01   | 0.070          |
| Ireland  | Northing | $H = -0.001N^2 + 0.334N + 221.44$                      | <0.01   | 0.027          |
|          | Easting  | $H = 219.79e^{-0.001E}$                                | <0.01   | 0.082          |
|          | Dist.    | Not stat. sig.   | 0.268   | n/a            |
|          | DistW    | $H = 0.002\text{distW}^2 + 0.108\text{distW} + 264.13$ | <0.01   | 0.049          |
| Wales    | Northing | $H = 93.574e^{0.003N}$                                 | <0.01   | 0.213          |
|          | Easting  | $H = 1832.8e^{-0.007E}$                                | <0.01   | 0.133          |
|          | Dist.    | $H = 284.22e^{-0.009\text{dist}}$                      | <0.01   | 0.080          |
|          | DistW    | $H = 271.14e^{-0.003\text{distW}}$                     | <0.01   | 0.102          |
| England  | Northing | Not stat. sig.   | 0.024   | n/a            |
|          | Easting  | Not stat. sig.   | 0.361   | n/a            |
|          | Dist.    | Not stat. sig.   | 0.571   | n/a            |
|          | Dist. W  | Not stat. sig.   | 0.694   | n/a            |

609  
610  
611  
612  
613  
614  
615  
616  
617  
618  
619  
620  
621  
622  
623  
624  
625  
626